Identification of candidate genes for adult plant stripe rust resistance transferred from Aegilops ventricosa 2NvS into wheat via fine mapping and transcriptome analysis

Yuqi Wang
Sichuan Agricultural University - Chengdu Campus
Mengru Gao
Sichuan Agricultural University - Chengdu Campus
Yunfeng Jiang
Sichuan Agricultural University - Chengdu Campus
Wuzhou Huang
Sichuan Agricultural University - Chengdu Campus
Xin Zhao
Sichuan Agricultural University - Chengdu Campus
Wei Zhu
Sichuan Agricultural University - Chengdu Campus
Hao Li
Sichuan Agricultural University - Chengdu Campus
Yi Wang
Sichuan Agricultural University - Chengdu Campus
Jian Zeng
Sichuan Agricultural University - Chengdu Campus
Dandan Wu
Sichuan Agricultural University - Chengdu Campus
Yuming Wei
Sichuan Agricultural University - Chengdu Campus
Yonghong Zhou
Sichuan Agricultural University - Chengdu Campus
Youliang Zheng
Sichuan Agricultural University - Chengdu Campus
Peng Zhang
The University of Sydney
Guoyue Chen
Sichuan Agricultural University - Chengdu Campus https://orcid.org/0000-0001-7710-1684
Houyang kang
houyang.kang@sicau.edu.cn
Sichuan Agricultural University https://orcid.org/0000-0002-0561-5413

Research Article

Keywords: adult plant resistance, Aegilops ventricosa, stripe rust, fine mapping, transcriptome

Posted Date: October 28th, 2023

DOI: https://doi.org/10.21203/rs.3.rs-3470403/v1

Version of Record: A version of this preprint was published at Theoretical and Applied Genetics on May 1st, 2024. See the published version at https://doi.org/10.1007/s00122-024-04620-1.

Abstract

The 2N^{v}S translocation from *Aegilops ventricosa*, known for its resistance to various diseases, has been pivotal in global wheat breeding for more than three decades. Here we identified an adult plant resistance (APR) gene in the 2N^{v}S segment in wheat line K13-868. Through fine mapping in a segregating near-isogenic line (NIL) derived population of 6,389 plants, the candidate region for the APR gene was narrowed down to between 19.36 Mb and 33 Mb in the Jagger v1.1 genome. Transcriptome analysis in NILs strongly suggested that this APR gene conferred resistance to stripe rust by triggering plant innate immune responses. Two disease resistance-associated genes within the candidate region, *TraesJAG2A01G041000* and *TraesJAG2A01G046200*, exhibited a stronger response to *Puccinia striiformis* f. sp. *tritici* (*Pst*) infection at the adult plant stage than at the seedling stage, indicating that they could be potential candidates for the resistance gene. Additionally, we developed a co-dominant InDel marker, *InDel_31.05*, for detecting this APR gene. Applying this marker showed that over one-half of the wheat varieties approved in 2021 and 2022 in Sichuan province, China, carry this gene. Agronomic trait evaluation of NILs indicated that the 2N^{v}S segment effectively mitigated the negative effects of stripe rust on yield without affecting other important agronomic traits. This study provided valuable insights for cloning and breeding through the utilization of the APR gene present in the 2N^{v}S segment.

Key message

An adult plant gene for resistance to stripe rust was narrowed down to the proximal one-third of the 2N^{v}S segment translocated from *Aegilops ventricosa* to wheat chromosome arm 2AS, and two candidate genes were identified showing a stronger response at the adult plant stage compared to the seedling stage.

Introduction

Stripe rust caused by *Puccinia striiformis* f. sp. *tritici* (*Pst*), is one of the most devastating diseases of wheat worldwide (Wellings 2011). Breeding for resistance has long been recognized as the most effective and environmentally friendly approach to control stripe rust (Chen 2013). Over the years, 86 officially cataloged and numerous provisionally named stripe rust resistance genes (*Yr* genes) and quantitative trait loci (QTL) were identified (McIntosh et al. 2020; Zhu et al. 2023). Many of these resistance genes have been successfully incorporated into modern wheat varieties (McIntosh et al. 2017). However, due to continually evolving pathogen races capable of overcoming deployed resistance genes, many *Yr* genes are no longer effective against current prevalent races (Chen and Kang 2017; Han et al. 2015). Furthermore, some molecular markers lack tight genetic linkage with target genes, making them unsuitable for marker-assisted breeding. Therefore, there is a need for continuing identification and characterization of sources of durable resistance for breeding (Chen and Kang 2017).

Wild relatives represent invaluable reservoirs of genetic diversity for bread wheat (*Triticum aestivum*). Serving as secondary and tertiary gene pools of wheat, they have contributed numerous invaluable disease resistance genes. Genetic diversity in modern wheat has been enriched by successfully introgression of genes from more than 52 Triticeae species across 13 genera (Wulff and Moscou 2014). A notable example is *Aegilops ventricosa*, a tetraploid species with a genome constitution of 2n = 4x = 28 (N^{v}N^{v}D^{v}D^{v}). The 2N^{v}S translocation segment from *Ae. ventricosa* has been recognized for harboring important resistance genes against multiple wheat diseases including stripe rust, leaf rust, stem rust, wheat blast, and cereal cyst nematode (Bariana and McIntosh 1993; Cruz et al. 2016; Jahier et al. 2001). This segment, first integrated into the wheat cultivar VPM1, has significantly influenced global wheat breeding programs since the early 1990s. This influence is particularly evident in the USA regional winter wheat program, the

CIMMYT spring wheat breeding program, as well as the wheat breeding program in Sichuan province, China (Gao et al. 2021; Xi et al. 2021).

The $2N^vS$ segment is known to harbor an all-stage resistance gene *Yr17*. However, with the emergence and spread of *Yr17*-virulent races since the 1990s in China, wheat cultivars carrying the $2N^vS$ translocation segment are susceptible to the most prevalent races at the seedling stage (Liu et al. 2018; Zeng et al. 2015). Nevertheless, several studies have shown that such cultivars retained resistance during the adult plant stage. For instance, the extensively cultivated U.S. variety 'Jagger', which carries the $2N^vS$ translocation segment, displayed moderate susceptibility at the seedling stage but was resistant at the adult plant stage against the same *Pst* races (Bayles and Herron 1987). Moreover, QTL analyses conducted on crosses involving wheat varieties such as Madsen (Liu et al. 2018), Mianyang351-15 (Gebrewahid et al. 2020), Borlaug 100 (Ye et al. 2022) and P2711 (Farzand et al. 2022), which all carry the $2N^vS$ translocation segment demonstrated the presence of a major-effect QTL for adult plant resistance within or near the $2N^vS$ region, following the infection with *Yr17*-virulent races. This has led to the hypothesis that, in addition to *Yr17*, the $2N^vS$ segment might harbor an adult plant resistance (APR) gene. Supporting this hypothesis, a recent study by Li et al. (2023) successfully identified a high-temperature adult plant (HTAP) resistance gene within the $2N^vS$ region by using AvSYr17NIL mutant lines. However, despite the availability of a high-quality genome sequence of the $2N^vS$ segment, the suppression of recombination between the $2N^vS$ segment and the homoeologous chromosome region of wheat 2AS makes precise mapping of this APR gene a challenge. As a result, the region of the candidates for the APR gene spans the full length of the $2N^vS$ segment, approximately 33 Mb in size.

In this study, we identified an APR gene in the $2N^vS$ segment in wheat line K13-868 that exhibited a high degree of APR to stripe rust. To further characterize this APR gene, we developed a near-isogenic line (NIL) population for stripe rust resistance following the heterogeneous inbred family (HIF) method (Tuinstra et al. 1997). The primary objectives of the study were: (1) to obtain recombinants involving the $2N^vS$ segment based on a large NIL population, aiming to narrow down the candidate gene region for the APR gene; (2) to investigate the mechanisms underlying the APR based on transcriptome analysis of the NILs; and (3) to identify candidate genes by integrating results from fine mapping and transcriptome analysis.

Materials and methods

Plant materials

A total of 214 recombinant inbred lines (RILs) from a cross between resistant line K13-868 and susceptible line SY95-71 were used to map QTL for stripe rust resistance. NILs for the $2N^vS$ segment were generated from a heterozygous line selected from the F_5 RIL population following the HIF method. Using the marker *InDel_2.87*, 42 plants that were segregating for the $2N^vS$ segment, were selected to develop a large NIL-derived population of 6,389 plants. The wheat line Yr17/6*Avocet S (AvS) served as the resistant control harboring the $2N^vS$ segment, and AvS and Mingxian 169 (MX169) were used as susceptible controls. A collection of 259 wheat cultivars from the Sichuan region, dating from 1996 onwards, was used to analyze the frequency of the $2N^vS$ segment in Sichuan wheat varieties/advanced lines.

Greenhouse evaluation

Both seedling and adult plants of K13-868, SY95-71, NILs, and MX169 were evaluated against *Pst* races CYR34 in the greenhouse. Seeds were grown in 10×10 cm pots at four plants per pot. Each line was sown in two pots for different temperature profile tests every week for four weeks until the plants spanning the 2nd to 5th leaf stages, all plants at four stages were inoculated. Inoculated plants were placed in a dew chamber at 10 ℃ for 24 h without light and then moved to two different growth chambers with a diurnal cycle of 16 h light/8 h darkness. One chamber simulated a low-temperature (LT) profile ranging from 10 to 15°C, while the other simulated a high-temperature (HT) profile, ranging from 10 to 30°C. The temperature was gradually changed from the lowest at 2 am to the highest at 2 pm (Chen 2013). Infection types (IT) were recorded at 18 to 21 days post-inoculation using a 0–9 scale (Line and Qayoum 1992).

Field experiments

In 2019–2020, the 214 F_5 (K13-868 × SY95-71) RILs and parents were evaluated for stripe rust response across three locations in Sichuan: Chongzhou (CZ; 30°32′N, 103°38′E), Pixian (PX; 103°89′E, 30°810′N) and Wenjiang (WJ; 103°41′E, 30°360′N) during 2019–2020. The same set, advanced to F_6, was evaluated again at CZ in the 2020–2021 crop season. Fine mapping NIL-derived population was planted at CZ in 2020–2023, and 46 recombinant lines were planted in rows at CZ in 2021–2022. The field plots were artificially inoculated using mixed current predominant *Pst* races in China (including CYR32, CYR33, CYR34, G22-14, Su11-4, Su11-5, and Su11-7) in the fields. Fifteen seeds of each line were planted in a 1.5 m row with 25 cm between rows. The susceptible check AvS was planted every 20 rows. The plants were recorded for infection type (IT) and Disease severity (DS), when AvS displayed 80% or more in severity. ITs were recorded using the 0–9 scale of Line and Qayoum, (1992). DS was scored based on the modified Cobb scale (Peterson et al. 1948) and the final disease severity (FDS) was used in phenotypic analysis.

DNA isolation, KASP and InDel marker development, and molecular mapping

Genomic DNA was extracted from leaf samples of each plant using the CTAB method (Stewart 1993). Exome capture sequencing of the resistant parent K13-868 and susceptible parent SY95-71 followed the protocol described by Dong et al. (2020). A subset of SNPs and InDels polymorphic between the parents in the target region was selected for conversion to KASP and InDel markers. The procedures of SNP conversion to KASP markers and selective KASP assay were described previously (Ramirez-Gonzalez et al. 2015). InDel markers were designed by Primer3Plus (https://www.primer3plus.com/). Linkage analysis was performed using JoinMap v4.0 (Kyazma BV, Wageningen, The Netherlands) (Van Ooijen 2006) with a LOD threshold of 3.0. The Kosambi mapping function (Kosambi 1944) was used to convert the recombination fractions to centimorgans. Mapping of QTL was performed using QTL IciMapping v4.2 based on the inclusive composite interval mapping (Wang et al. 2019).

RNA isolation and transcriptome sequencing analysis

Plants of the NILs at four growth stages, from the 2nd to 5th leaf stages, were inoculated with fresh *Pst* race CYR34. Plants sprayed with isododecane served as a mock control. RNA samples for Illumina sequencing were harvested at 3 days post inoculation (dpi) from *Pst*-inoculated and mock-inoculated NIL-R and NIL-S. Three biological replicates were collected from each inoculated and mock-inoculated plant. Total RNA was extracted using TRIzol reagent (Invitrogen, Carlsbad, CA, USA) according to the manufacturer's instructions. In total, 18 constructed libraries were sequenced on the Illumina NovaSeq 6000 platform at Beijing Berry Genomics (Beijing, China) to generate 150 bp paired-end sequences. Sequence quality assessment, quality trimming, and RNA-seq analysis were performed using CLC Genomics Workbench 12.0 software with default parameters (Liu and Di 2020). The generated clean reads were aligned to the wheat "Jagger" reference genome (Walkowiak et al. 2020). The expression level of each gene was

calculated using FPKM (Fragments per Kilobase of exon per million fragments Mapped). An absolute value of |log2FoldChange| ≥ 1 and *p-value* < 0.05 were considered as differentially expressed genes (DEGs). DEGs were used for Gene Ontology (GO) enrichment analysis. Triticeae-GeneTribe (http://wheat.cau.edu.cn/TGT/, Chen et al. 2020) was used in the GO term enrichment analysis.

Eight DEGs were randomly selected and assessed using reverse transcription quantitative PCR (RT-qPCR). Gene-specific primers were designed by Primer3Plus (https://www.primer3plus.com/). EF-1α, the elongation factor of wheat, was used as the internal reference gene. RNA isolation, cDNA synthesis, and RT-qPCR analysis were performed as described in Wang et al. (2010). The relative expression of each gene was calculated using the comparative CT method ($2^{-\Delta\Delta CT}$) (Livak and Schmittgen 2001). RT-qPCR of each sample was performed three times and each treatment was amplified in triplicate.

Agronomic traits assessment under stripe rust stress

The NILs were evaluated for agronomic traits under stripe rust stress in the 2021–2022 and 2022–2023 growing seasons at CZ and WJ. Twenty seeds of each NIL were evenly planted in a 2-m row with 0.3 m between rows. Each NIL was planted in three rows and evaluated for six agronomic traits: plant height (PH), spike length (SL), tiller number (TN), spike number (SN), grain number per spike (GNPS), and thousand kernel weight (TKW). All traits were measured on five randomly selected plants for each NIL at harvest. Kernel length (KL) and kernel width (KW) were also assessed using 15 randomly selected seeds of NIL-R and NIL-S, respectively.

Statistical analysis

Mean IT and FDS of $F_{5:6}$ RILs were used to examine the variance within individual environments. For each trait, the best linear unbiased prediction (BLUP) values were calculated across environments using the ANOVA function in IciMapping V4.2 software assuming fixed effects for the genotype. Student's t-tests ($P < 0.05$ and 0.01) were conducted with Excel 2016 (Microsoft, Redmond, WA, USA) to evaluate the significance of differences between the two groups (Mishra et al. 2019).

Results

Mapping an APR gene on 2N^{v}S segment in wheat line K13-868

K13-868 seedlings were susceptible (IT 8) to race CYR34 in the greenhouse (Fig. 1a). However, in field environments, this line exhibited a high level of adult plant resistance (IT 3) to stripe rust when exposed to mixed races (Fig. 1b, c). IT and FDS for each line in the RIL population derived from the cross K13-868 × SY95-71, along with parental lines, were assessed across four different environments in 2020 and 2021 (Table S1). The frequency distribution for IT and FDS displayed characteristics typical of a quantitative trait (Fig. 1d, e). Subsequently, using closely linked molecular markers or functional markers for stripe rust resistance genes, commonly used *Yr* genes in Chinese wheat varieties were tested in this line (Table S2). The *Yr17* linked marker *SC_372* was detected in K13-868, suggesting it carried the 2N^{v}S segment. To validate the genetic effect of the 2N^{v}S segment on the adult plant stripe rust resistance of K13-868, *SC_372* and six newly developed linked markers (Table S3) covering physical regions from 2.87 to 43.76 Mb on chromosome 2AS, were used for genotyping 214 $F_{5:6}$ plants from K13-868 × SY95-71 to construct a genetic map spanning 25.60 cM (Table S4). Using the IT and FDS values of the four sets from the F_5 and F_6 populations (CZ2020, PX2020, WJ2020, and CZ2021) and their BLUP values (Table S1), a major QTL was identified consistently across all tests. This QTL was linked with markers *InDel_2.87* and *KP2A_34.29*, explaining 18.55 to 33.16% of the phenotypic variation with LOD scores ranging from 9.69 to 18.73 (Fig. 1f; Table S5). Evidently, an APR locus exists in the 2N^{v}S

segment of the wheat line K13-868, conferring effective resistance against the current predominant *Pst* races of China.

Development and evaluation of NILs for stripe rust response

A pair of NILs for the 2N^{v}S segment were selected from the progeny of a heterozygous F_5 line, which was from the RIL population created by crossing K13-868 with SY95-71. Seedling tests showed that both NIL-R and NIL-S plants were susceptible to CYR34 (Fig. 2a). However, at the adult plant stage, the NIL-R plants (IT 5) exhibited greater resistance to mixed *Pst* races compared to the NIL-S plants (IT 8) (Fig. 2b). To better understand the dynamics of resistance conferred by the APR gene, we evaluated the response at four growth stages (ranging from the 2nd to 5th leaf stages) to race CYR34 under two temperature regimes: Low temperature (LT, 10–15°C) and High temperature (HT, 10–30°C) in the greenhouse (Fig. 2a). In the LT test, both K13-868 and NIL-R were highly susceptible to CYR34 until the 5th leaf stage when resistance was seen. In contrast, SY95-71 and NIL-S were susceptible at all four growth stages. Under the HT test, both K13-868 and NIL-R began to display resistance to CYR34 by the 4th leaf stage. These results further confirmed that the stripe rust resistance originating from the 2N^{v}S segment in K13-868 was more effective under high temperature condition.

Fine mapping of the APR gene on the 2N^{v}S segment using a large NIL-derived population

To narrow down the candidate gene region for the APR gene in the 2N^{v}S segment, a large NIL-derived population of 6,389 plants was used for screening recombinants within the 2N^{v}S segment region. In total, 22 molecular markers, located between 0.16 Mb and 31.05 Mb on the 2N^{v}S segment (Table S3), were developed to precisely identify recombinant events. Although the 2N^{v}S segment rarely recombines with the 2AS chromosome on wheat, we fortuitously identified 22 recombinants within this 33 Mb physical interval. Using these markers, we genotyped the 22 recombinants on the 2N^{v}S segment (Table S6) and refined the location of the APR gene.46 families of 5 recombinants with critical recombination events were planted again in 2021–2022 (Table S7), providing additional support to the proposed location of the APR gene. We found that the recombination events were not randomly distributed across the 2N^{v}S segment, but enriched in certain regions, e.g., the crossovers in the 14 lines were between 12.38 and 14.91 Mb. Based on the phenotypic identification of critical recombinants and families, we narrowed down the candidate gene region for the APR gene to 19.36-33 Mb in the Jagger v1.1 genome (Fig. 3).

RNA-seq analysis of NILs for stripe rust response during Pst infection

We conducted transcriptome sequencing of NILs inoculated with the fresh rust of *Pst* race CYR34 at both the 2nd and 5th leaf stages to investigate the key gene responses and pathways involved in the APR on the 2N^{v}S segment. Leaves of NIL-R2, NIL-R5, and NIL-S5 for Illumina RNA sequencing were harvested at 3 dpi from *Pst*-inoculated and mock-inoculated plants. A total of 76.65 million 150-bp paired-end reads were obtained for 18 samples. After adapter trimming and filtering low-quality reads, a total of 74.26 million clean reads remained with an average Q20 of 96.96% and Q30 of 92.33% (Table S8). The number of reads from each sample ranged from 9.98 to 15.88 GB. The filtered clean reads were mapped to the Jagger Reference genome, and the mapping ratio of clean reads reached 96.29–97.47% (Table S8). Most reads for all samples were successfully mapped, and sequences sufficiently captured most of the expressed genes. Using RT-qPCR analysis on eight randomly selected genes, we verified that the results were consistent with the transcriptome data (Fig. S1; Table S9).

Totals of 8,513, 7,685, and 4,747 DEGs were identified in NIL-R5, NIL-S5, and NIL-R2, respectively (Fig. 4a, b). Among them, 6,570, 6,603, and 719 DEGs were up-regulated, whereas 1,943, 1,082, and 4,028 DEGs were down-regulated in NIL-R5, NIL-S5, and NIL-R2, respectively. Twenty-five up-regulated DEGs were detected only in NIL-R5. Most of them encoded proteins related to disease resistance, e.g., *TraesJAG6B01G518500* encodes chitin elicitor receptor kinase 1, *TraesJAG2D01G557400* encodes wall-associated receptor kinase-like 8, and *TraesJAG2A01G490300* encoding probable L-type lectin-domain containing receptor kinase S.5 (Fig. 4c).

These DEGs in NIL-R5, NIL-S5, and NIL-R2 plants were further subjected to GO analysis. This analysis revealed that 248, 185, and 56 terms related to biological processes were enriched (FDR < 0.05) in up-regulated DEGs of NIL-R5, NIL-S5, and NIL-R2, respectively, whereas 163, 101, and 202 functional biological process categories were enriched in down-regulated DEGs. GO terms enriched in up-regulated DEGs of NIL-R5 were more abundant than in NIL-S5 and NIL-R2 (Fig. S2a-f). Specifically, plant immune-related pathways, including calmodulin binding (GO:0005516), protein kinase activity (GO:0004672), transmembrane receptor protein serine/threonine kinase activity (GO:0004675), and plant-type hypersensitive response (GO:0009626), were more enriched in DEGs of NIL-R5 compared to NIL-S5 and NIL-R2 (Fig. 4d, e).

Candidate genes for the APR gene in the 2N^{v}S segment

The candidate region for the APR gene on the 2N^{v}S segment, spanning from 19.36 Mb to 32.53 Mb on the 2AS chromosome of the Jagger reference genome, includes 266 high-confidence genes. Based on the RNA-seq data and applying the threshold (RPKM ≥ 1, observed at least once at either seedling or adult plant stages of NIL-R during Mock and *Pst* infection), 49 expressed genes were identified within the candidate gene region (Fig. 5a). Eleven DEGs were identified between mock and *Pst* infections in the adult plant stage of NIL-R. Among these, only two genes exhibited expression levels more than twice as high at the adult plant stage against *Pst* infection as the seedling stage (Fig. 5b). According to the gene annotations provided by the Triticeae-Gene Tribe (TGT; http://wheat.cau.edu.cn/TGT/), the two genes, *TraesJAG2A01G041000* and *TraesJAG2A01G046200*, encode for L-type lectin-domain containing receptor kinase SIT2 and Disease resistance protein RPM1, respectively.

Marker-based detection of the 2N^{v}S segment distribution in Sichuan wheat cultivars

Compared to the dominant marker *SC_372* for detecting the 2N^{v}S segment, the five co-dominant InDel markers developed in this study differentiate the 2N^{v}S segment from its homoeologous wheat 2AS chromosome. This advances the marker-assisted selection (MAS) of the 2N^{v}S segment, especially enhancing the efficiency of heterozygote genotyping screening MAS. Utilizing the newly developed marker *InDel_31.05*, we analyzed the 2N^{v}S segment distribution in 259 wheat varieties from the Sichuan region released after 1996 (Fig. 6a; Table S10) and identified 106 cultivars carrying the 2N^{v}S segment. Notably, of 81 varieties selected from years 2021 and 2022, 42 were detected with the segment, indicating a rise in proportion to 52% in the recent two years (Fig. 6b). Based on the BLUP values of FDS of the 142 varieties (Ye et al. 2019), clearly, the varieties that carried the 2N^{v}S segment showed a significantly lower FDS than those without it, and the mean BLUP_FDS values of the varieties carrying it were reduced by 41% (Fig. 6c, d).

Agronomic trait evaluation of NILs for the 2N^{v}S segment

During the 2021–2022 and 2022–2023 growing seasons in CZ and WJ, agronomic traits of NIL-R and NIL-S lines were compared under an equal mix of *Pst* inoculated conditions (Fig. 7). The presence of the $2N^vS$ segment resulted in significantly higher ($P < 0.05$) values for grain number per spike (GNPS) in CZ2022, WJ2022 and CZ2023, thousand kernel weight (TKW) ($P < 0.01$) in WJ2022, kernel width (KW) ($P < 0.01$) in CZ2023. On the other hand, plant height (PH), spike length (SL), tiller number (TN), spike number (SN), and kernel length (KL) were not significantly different between the NIL-R and NIL-S plants. These findings demonstrated that the $2N^vS$ segment offset the adverse impacts of stripe rust on yield, without negatively influencing the evaluated agronomic traits.

Discussion

In our study, we identified an APR gene on the $2N^vS$ segment of the wheat line K13-868. Multi-year field trials confirmed that this gene exhibits moderate resistance to prevalent *Pst* races in China. To further elucidate the characteristics of this APR gene, we developed a NIL population for stripe rust resistance using the HIF method (Tuinstra et al. 1997). The evaluation revealed that the APR gene conferred resistance at the 5th leaf stage, with enhanced resistance at high temperatures, classifying it as an HTAP resistance gene. Li et al. (2023) successfully identified an HTAP resistance gene within the $2N^vS$ regions using AvSYr17NIL mutant lines, which was similar to our result. The suppression of recombination between the $2N^vS$ segment and the homoeologous chromosomal region of wheat 2AS makes precise mapping of this APR gene a challenge. However, in our study, we narrowed down the candidate gene region in the $2N^vS$ segment using a large NIL-derived population consisting of 6,389 plants for fine mapping. Based on data from critical recombinants and their families, the APR gene was subsequently mapped to the proximal one third of the $2N^vS$ segment, corresponding to the region from 19.36 Mb to 33 Mb on chromosome 2A of the Jagger reference genome.

Cloning target genes from alien species using the conventional map-based approach is immensely challenging, primarily because of the suppressed recombination between the alien segment and its wheat homoeologous counterpart (Jayatilake et al. 2013; Xie et al. 2012). Nonetheless, several resistance genes from alien species have been successfully cloned to date. For instance, He et al. (2018) utilized *Bgt*-susceptible *Dasypyrum villosum* resources as a susceptible parent. By constructing a genetic population with resistant and susceptible *D. villosum*, they narrowed down *Pm21* to a 0.01 cM interval, which corresponds to a 112.5 kb genomic region in the model plant *Brachypodium distachyon*. In another study, Wang et al. (2020) overcame recombination suppression challenges for the map-based cloning of *Fhb7* from *Thinopyrum elongatum*. They employed a *ph1b*-based strategy, enhancing 7E and 7D recombination, and successfully mapped *Fhb7* to a 245-kb genomic region. Given the advancements in the next-generation sequencing and computational bioinformatics, the current predominant approach for cloning resistance genes from alien species use mutation and sequencing-based cloning. For instance, genes like *Sr26*, *Sr43*, and *Sr61* from *Thinopyrum ponticum*, *Sr62* from *Aegilops sharonensis*, and *Lr9* from *Aegilops umbellulata* have been successfully isolated and characterized via this methodology (Zhang et al. 2021; Yu et al. 2022, 2023; Wang et al. 2023). In this study, we also observed that due to recombination suppression, further narrowing down the candidate region by expanding the current genetic population might be challenging. Moving forward, the most suitable strategy for cloning this gene would be through mutation and sequencing-based cloning.

In addition to fine mapping, transcriptomic analysis of NILs provided critical clues in identifying the candidate genes. Of the over 300 resistance genes that have been cloned to date, the vast majority are either NBS-LRR or kinases, typically mediating resistance through the effector-triggered immunity (ETI) pathway (Ayliffe et al. 2022). Transcriptome analysis revealed that, compared with the seedling stage or NIL-S, several plant immunity-related pathways, like transmembrane receptor protein serine/threonine kinase activity and plant-type hypersensitive

response, were specifically upregulated in NIL-R at the adult plant stage. This suggests that ETI was activated only in the NIL-R at this stage. Such observations imply that the APR gene on the $2N^vS$ segment might confer adult plant resistance via innate immune pathways. This gene may belong to R gene types such as NBS-LRR or kinase genes that are specifically expressed at the adult plant stage. Further RNA-seq analysis in candidate regions indicated that among 266 genes in the candidate region, only 49 were expressed in NIL-R samples. From these, 11 genes exhibited differential expression at the adult plant stage of NIL-R in response to *Pst* infection. Crucially, two disease resistance-related genes, *TraesJAG2A01G041000* (L-type lectin-domain receptor kinase SIT2) and *TraesJAG2A01G046200* (Disease resistance protein RPM1) showed a stronger response to *Pst* infection at the adult plant stage compared to the seedling stage. We are currently undertaking validation work in mutants for these candidate genes.

The $2N^vS$ translocation known for its resistance to multiple diverse diseases (Bariana and McIntosh 1993; Cruz et al. 2016; Jahier et al. 2001), has played a pivotal role in global wheat breeding for over three decades. In a comprehensive study, Gao et al. (2021) traced the change in $2N^vS$ carrier frequency over 25 years in Kansas winter wheat and the CIMMYT spring wheat breeding program. They noted a significant rise in the $2N^vS$ frequency since the early 1990s, confirming its important role in wheat breeding. It is noteworthy that the $2N^vS$ frequency in recent years for both Kansas and CIMMYT breeding programs approached 80%. Similarly, our analysis of wheat varieties cultivated in Sichuan over the past two decades indicates a rising prevalence of the $2N^vS$ segment since 2001. Overall, over 40% of wheat varieties grown in Sichuan in the last 20 years harbor the $2N^vS$ segment, a number increased to 52% for the varieties approved in 2021 and 2022 in Sichuan. Therefore, the $2N^vS$ segment is experiencing significant positive selection pressure in global wheat breeding programs. Taking Sichuan as an example, as one of the most stripe rust-prone regions in China (Li and Zeng 2000), there has been a profound emphasis on stripe rust resistance in the breeding and approval of new wheat varieties over recent decades. Resistance evaluations using AvSYr17NIL indicated that the $2N^vS$ segment alone might not provide adequate protection against stripe rust pressure in the field. However, in wheat varieties cultivated in Sichuan, it is often combined with other stripe rust resistance genes, leading to robust resistance against prevalent *Pst* races in China. Additionally, the durable and non-race-specific resistance provided by the APR gene, combined with the beneficial agronomic effects of the $2N^vS$ segment, likely explains its rising frequency in the global wheat breeding over the past two decades.

Declarations

Conflict of interest The authors declare that they have no conflict of interest.

Funding This study was supported by the Major Program of National Agricultural Science and Technology of China (NK20220607), the National Natural Science Foundation of China (grant number 32272059, 31971883) and the Science and Technology Department of Sichuan province (grant numbers 2023NSFSC1995, 2022ZDZX0014, 2021YFYZ0002).

Availability of data and materials The datasets generated and analyzed in the present study are available from the corresponding author upon reasonable request. Exome capture sequencing (project number: PRJCA020498) and transcriptome data (project number: PRJCA020255) are available from the National Genomics Data Center (https://ngdc.cncb.ac.cn/). The materials, including the resistant Chinese wheat line ‘K13-868’, used in this study are deposited at Triticeae Research Institute, Sichuan Agricultural University, China.

Author contributions statement YQW, MRG and YFJ carried out the experiment, analyzed the data, and drafted the manuscript; WZH, XZ, WZ and HL carried out the phenotypic evaluation; YW, JZ, DDW, YMW, YHZ and YLZ provided resources and technique guidance; PZ, GYC and HYK designed and carried out the experiment, formulated the questions, analysed the data and revised the manuscript. All authors have reviewed and approved the final manuscript.

Acknowledgments The authors are grateful to Prof. Qiu-Zhen Jia from Plant Protection Research Institute, Gansu Academy of Agricultural Sciences, Lanzhou, P. R. China for providing the stripe rust races and Prof. Robert McIntosh, University of Sydney, Australia, for critical review of the manuscript.

References

1. Ayliffe M, Luo M, Faris J, Lagudah E (2022) Disease Resistance. In: Reynolds, M.P., Braun, HJ. (eds) Wheat Improvement. Springer, Cham. https://doi.org/10.1007/978-3-030-90673-3_19
2. Bariana HS, McIntosh RA (1993) Cytogenetic studies in wheat. XV. Location of rust resistance genes in VPMl and their genetic linkage with other disease resistance genes in chromosome 2A. Genome 36:476–482
3. Bayles RA, Herron CM (1987) Yellow rust of wheat. Pages 15-20 in UK Cereal Pathogen Virulence Report for 1986. NIAB, Cambridge, England.
4. Chen X (2013) High-temperature adult-plant resistance, key for sustainable control of stripe rust. Am J Plant Sci 4:608–627
5. Chen XM, Kang ZS (2017) Stripe rust. Springer Netherlands, pp 353–618
6. Chen YM, Song WJ, Xie XM, Wang ZH, Guan PF, Peng HR, Jiao YN, Ni ZF, Sun QX, Guo WL (2020) A collinearity-incorporating homology inference strategy for connecting emerging assemblies in the triticeae tribe as a pilot practice in the plant pangenomic era. Mol Plant 13:1694–1708
7. Cruz CD, Peterson GL, Bockus WW, Kankanala P, Dubcovsky J, Jordan KW, Akhunov E, Chumley F, Baldelomar FD, Valent B (2016) The 2NS translocation from *Aegilops ventricosa* confers resistance to the *Triticum* pathotype of *Magnaporthe oryzae*. Crop Sci 56:990–1000
8. Dong CH, Zhang LC, Chen ZX, Xia C, Gu YQ, Wang JR, Li DP, Xie ZC, Zhang Q, Zhang XY, Gui LX, Liu X, Kong XY (2020) Combining a new exome capture panel with an effective varBScore algorithm accelerates BSA-based gene cloning in Wheat. Front Plant Sci 11:1249
9. Farzand M, Dhariwal R, Hiebert CW, Spaner D, Randhawa HS (2022) QTL mapping for adult plant field resistance to stripe rust in the AAC Cameron/P2711 spring wheat population. Crop Sci 62:1088–1106
10. Gao LL, Koo DH, Juliana P, Rife T, Singh D, Lemes da Silva C, Lux T, Dorn KM, Clinesmith M, Silva P, Wang X, Spannagl M, Monat C, Friebe B, Steuernagel B, Muehlbauer GJ, Walkowiak S, Pozniak C, Singh R, Stein N, Mascher M, Fritz A, Poland J (2021) The *Aegilops ventricosa* $2N^vS$ segment in bread wheat: cytology, genomics and breeding. Theor Appl Genet 134:529–542
11. Gebrewahid TW, Zhou Y, Zhang P, Ren Y, Gao P, Xia X, He Z, Li Z, Liu D (2020) Mapping of stripe rust and leaf rust resistance quantitative trait loci in the Chinese spring wheat line Mianyang351-15. Phytopathology 110:1074–1081
12. Han DJ, Wang QL, Chen XM, Zeng QD, Wu JH, Xue WB, Zhan GM, Huang LL, Kang ZS (2015) Emerging *Yr26*-virulent races of *Puccinia striiformis* f. sp. *tritici* are threatening wheat production in the Sichuan Basin, China. Plant Dis 99:754–760

13. He H, Zhu S, Zhao R, Jiang Z, Ji Y, Ji J, Qiu D, Li H, Bie T (2018) *Pm21*, encoding a typical CC-NBS-LRR protein, confers broad-spectrum resistance to wheat powdery mildew disease. Mol Plant 11:879–882
14. Jahier J, Abelard P, Tanguy M, Dedryver F, Rivoal R, Khatkar S, Bariana HS, Koebner R (2001) The *Aegilops ventricosa* segment on chromosome 2AS of the wheat cultivar 'VPM1' carries the cereal cyst nematode resistance gene *Cre5*. Plant Breed 120:125–128
15. Jayatilake DV, Tucker EJ, Bariana H, Kuchel H, Edwards J, McKay AC, Chalmers K, Mather DE (2013) Genetic mapping and marker development for resistance of wheat against the root lesion nematode *Pratylenchus neglectus*. BMC Plant Biol 13:230
16. Kosambi DD (1943) The estimation of map distances from recombination values. Ann Eugen 12:172–175
17. Li Y, Liu L, Wang M, Ruff T, See DR, Hu X, Chen X (2023) Characterization and molecular mapping of a gene conferring high-temperature adult-plant resistance to stripe rust originally from *Aegilops ventricosa*. Plant Dis 107:431–442
18. Li ZQ, Zeng SM (2000) 'Wheat rusts in China.' China Agricultural Press, China
19. Line RF, Qayoum A (1992) Virulence, aggressiveness, evolution, and distribution of races of *Puccinia striiformis* (the cause of stripe rust of wheat) in North America, 1968-1987. Department of Agriculture Technical Bulletin U.S. No. 1788. http://naldc.nal.usda.gov/download/CAT92983836/PDF
20. Liu CH, Di YP (2020) Analysis of RNA sequencing data using CLC genomics workbench. In Molecular Toxicology Protocols. Methods in Molecular Biology Humana, Vol 2102. Humana, New York, pp 61–113
21. Liu L, Wang MN, Feng JY, See DR, Chao SM, Chen XM (2018) Combination of all-stage and high-temperature adult-plant resistance QTL confers high-level, durable resistance to stripe rust in winter wheat cultivar Madsen. Theor Appl Genet 131:1835–1849
22. Livak KJ, Schmittgen TD (2001) Analysis of relative gene expression data using real-time quantitative PCR and the $2^{-\Delta\Delta CT}$ method. Methods 25:402–408
23. McIntosh RA, Dubcovsky J, Rogers WJ, Morris C, Appels R, Xia XC (2017) Catalogue of gene symbols for wheat: 2017 Supplement. http:// shigen.nig.ac.jp/wheat/komugi/genes/macgene/supplement2017.pdf
24. McIntosh RA, Dubcovsky J, Rogers WJ, Xia XC, Raupp WJ (2020) Catalogue of Gene Symbols for Wheat: 2020 Supplement. https://wheat.pw.usda.gov/GG3/sites/default/files/Catalogue%20of%20Gene%20Symbols%20for%20Wheat%20-%20supplement2020.pdf Mishra P, Singh U, Pandey CM, Mishra P, Pandey G (2019) Application of student's t-test, analysis of variance, and covariance. Ann Card Anaesth 22:407–411
25. Peterson RF, Campbell AB, Hannah AE (1948) A diagrammatic scale for estimating rust intensity on leaves and stems of cereals. Can J Res 26:496–500
26. Ramirez-Gonzalez RH, Uauy C, Caccamo M (2015) PolyMarker: a fast polyploid primer design pipeline. Bioinform 31:2038–2039
27. Stewart CN, Via LE (1993) A rapid CTAB DNA isolation technique useful for RAPD fingerprinting and other PCR applications. Biotechniques 14:748–751
28. Tuinstra MR, Ejeta G, Goldsbrough PB (1997) Heterogeneous inbred family (HIF) analysis: a method for developing near isogenic lines that differ at quantitative trait loci. Theor Appl Genet 95:1005–1011
29. Van Ooijen JW (2006) JoinMap® 4.0: Software for the calculation of genetic linkage maps in experimental populations. Kyazma BV, Wageningen, The Netherlands
30. Walkowiak S, Gao L, Monat C et al (2020) Multiple wheat genomes reveal global variation in modern breeding. Nature 588:277–283

31. Wang H, Sun S, Ge W et al (2020) Horizontal gene transfer of *Fhb7* from fungus underlies Fusarium head blight resistance in wheat. Science 368:eaba5435
32. Wang JK, Li HH, Zhang LY, Meng L (2019) User's manual of QTL IciMapping ver. 4.2. Quantitative Genetics group, Institute of Crop Science, Chinese Academy of Agricultural Sciences CAAS/Genetic Resources Program, International Maize and Wheat Improvement Center CIMMYT, Beijing/Mexico City
33. Wang JR, Wang L, Gulden S, Rocheleau H, Balcerzak M, Hattori J, Cao W, Han F, Zheng YL, Fedak G, Ouellet T (2010) RNA profiling of fusarium head blight-resistant wheat addition lines containing the *Thinopyrum elongatum* chromosome 7E. Can J Plant Pathol 32:188–214
34. Wang Y, Abrouk M, Gourdoupis S, Koo DH, Karafiátová M, Molnár I, Holušová K, Doležel J, Athiyannan N, Cavalet-Giorsa E, Jaremko Ł, Poland J, Krattinge SG (2023) An unusual tandem kinase fusion protein confers leaf rust resistance in wheat. Nat Genet 55:914–920
35. Wellings CR (2011) Global status of stripe rust: a review of historical and current threats. Euphytica 179:129–141
36. Wulff BB, Moscou MJ (2014) Strategies for transferring resistance into wheat: from wide crosses to GM cassettes. Front Plant Sci 5:692
37. Xie WL, Ben-David R, Zeng B, Dinoor A, Xie CJ, Sun QX, Roder MS, Fahoum A, Fahima T (2012) Suppressed recombination rate in 6VS/6AL translocation region carrying the *Pm21* locus introgressed from *Haynaldia villosa* into hexaploid wheat. Mol Breed 29:399–412
38. Xi L, Wang YQ, Zhu W, Wang Y, Chen GY, Pu ZJ, Zhou YH, Kang HY (2021) Identification of resistance to wheat and molecular detection of resistance genes to wheat stripe rust of 78 wheat cultivars (lines) in Sichuan province. Acta Agronomica Sinica 47:1309–1323
39. Ye BW, Singh RP, Yuan C, Liu DM, Randhawa MS, Huerta-Espino J, Bhavani S, Lagudah E, Lan CX (2022) Three co-located resistance genes confer resistance to leaf rust and stripe rust in wheat variety Borlaug 100. Crop J 10: 490–497
40. Ye XL, Li J, Cheng YK, Yao FJ, Long L, Yu C, Wang YQ, Wu Y, Li J, Wang JR, Jiang QT, Li W, Ma J, Wei YM, Zheng YL, Chen GY (2019) Genome-wide association study of resistance to stripe rust (*Puccinia striiformis* f. sp. *tritici*) in Sichuan wheat. BMC Plant Biol 19:147
41. Yu G, Matny O, Champouret N et al (2022) *Aegilops sharonensis* genome-assisted identification of stem rust resistance gene *Sr62*. Nat Commun 13:1607
42. Yu G, Matny O, Gourdoupis S et al (2023) The wheat stem rust resistance gene *Sr43* encodes an unusual protein kinase. Nat Genet 55:921–926
43. Zeng QD, Shen C, Yuan FP, Wang QL, Wu JH, Xue WB, Zhan GM, Yao S, Chen W, Huang LL, Han DJ, Kang ZS (2015) The resistance evaluation of the *Yr* genes to the main prevalent pathotypes of *Puccinia striiformis* f. sp. *tritici* in China. Acta Phytopathologica Sinica 45:641–650
44. Zhang J, Hewitt TC, Boshoff WHP et al (2021) A recombined *Sr26* and *Sr61* disease resistance gene stack in wheat encodes unrelated NLR genes. Nat Commun 12:3378
45. Zhu ZW, Cao Q, Han DJ Wu JH, Wu L, Tong JY, Xu XW, Yan J, Zhang Y, Xu KJ, Wang FJ, Dong YC, Gao CB, He ZH, Xia XC, Hao YF (2023) Molecular characterization and validation of adult-plant stripe rust resistance gene *Yr86* in Chinese wheat cultivar Zhongmai 895. Theor Appl Genet 136:142

Figures

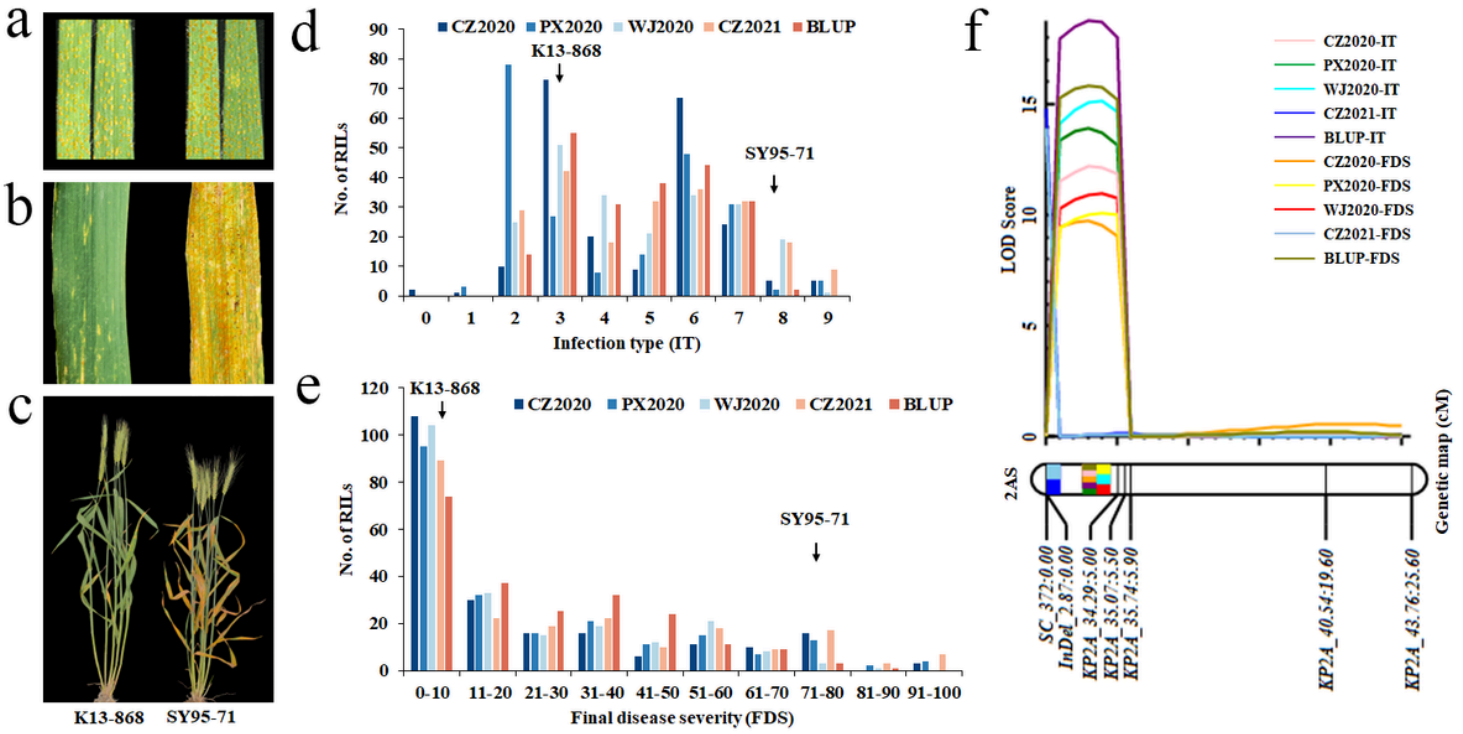

Figure 1

Stripe rust responses of the resistant (K13-868) and susceptible parent (SY95-71) following inoculation with CYR34 in the greenhouse (**a**) and mixture *Pst*at the adult plant stage in the field (**b, c**). Frequency distributions of the infection type (IT) (**d**) and final disease severity (FDS) (**e**) for the RIL population derived from K13-868 × SY95-71 at Chongzhou (CZ), Pixian (PX), Wenjiang (WJ) in 2020-2021 and BLUP values. QTL mapping of *QYr.868-2AS* for resistance to stripe rust on chromosome 2A based on IT and FDS data from the RILs derived from K13-868 × SY95-71 **(f)**.

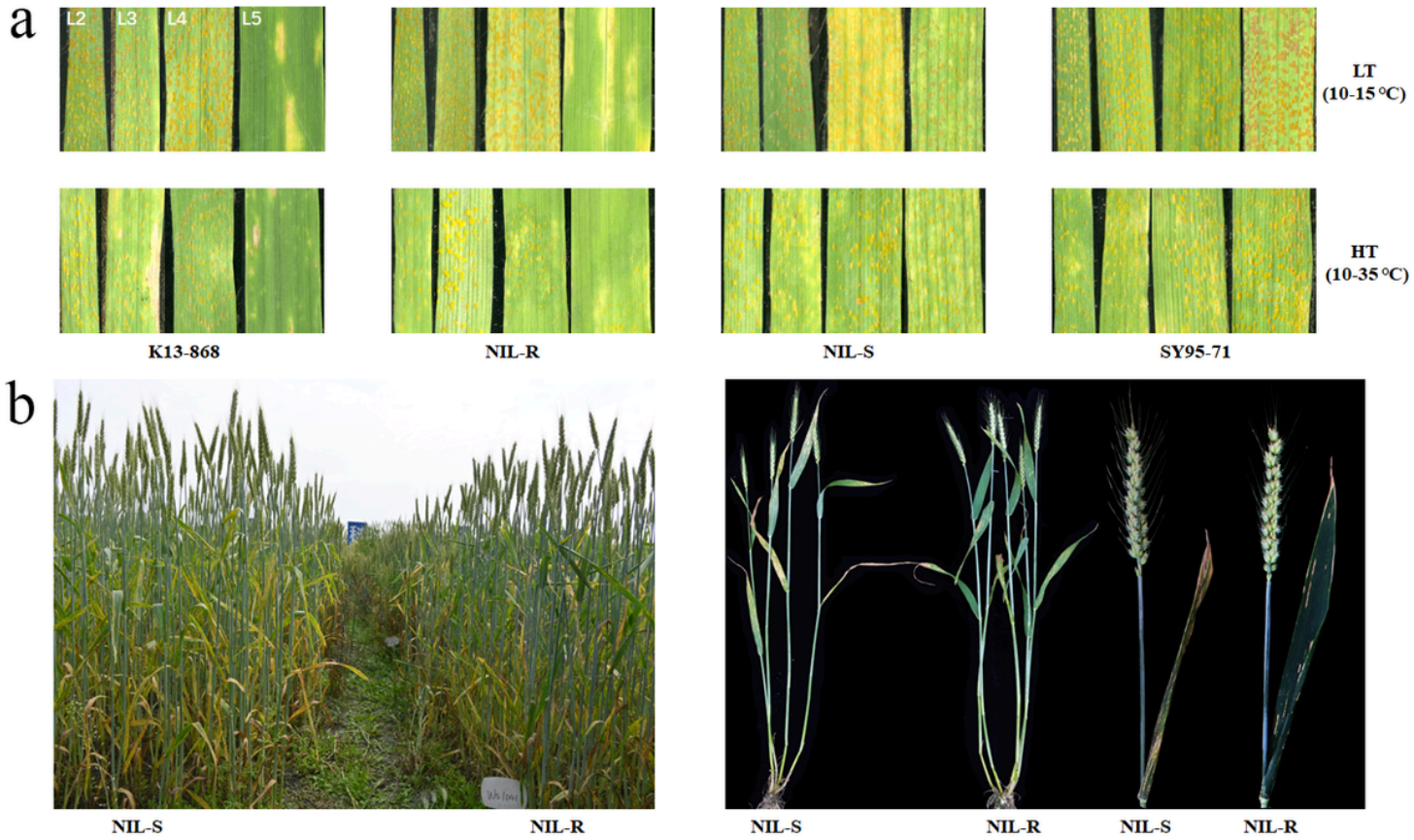

Figure 2

Stripe rust responses of K13-868, SY95-71 and NILs tested with CYR34 in low-temperature (LT, 10 – 15 °C) and high-temperature (HT, 10 – 30 °C) profiles at four growth stages (ranging from the 2nd to 5th leaf stages, L2-L5) in the greenhouse **(a)**, stripe rust response of NILs for stripe rust resistance with a mixture *Pst* at the adult plant stage in the field (**b**).

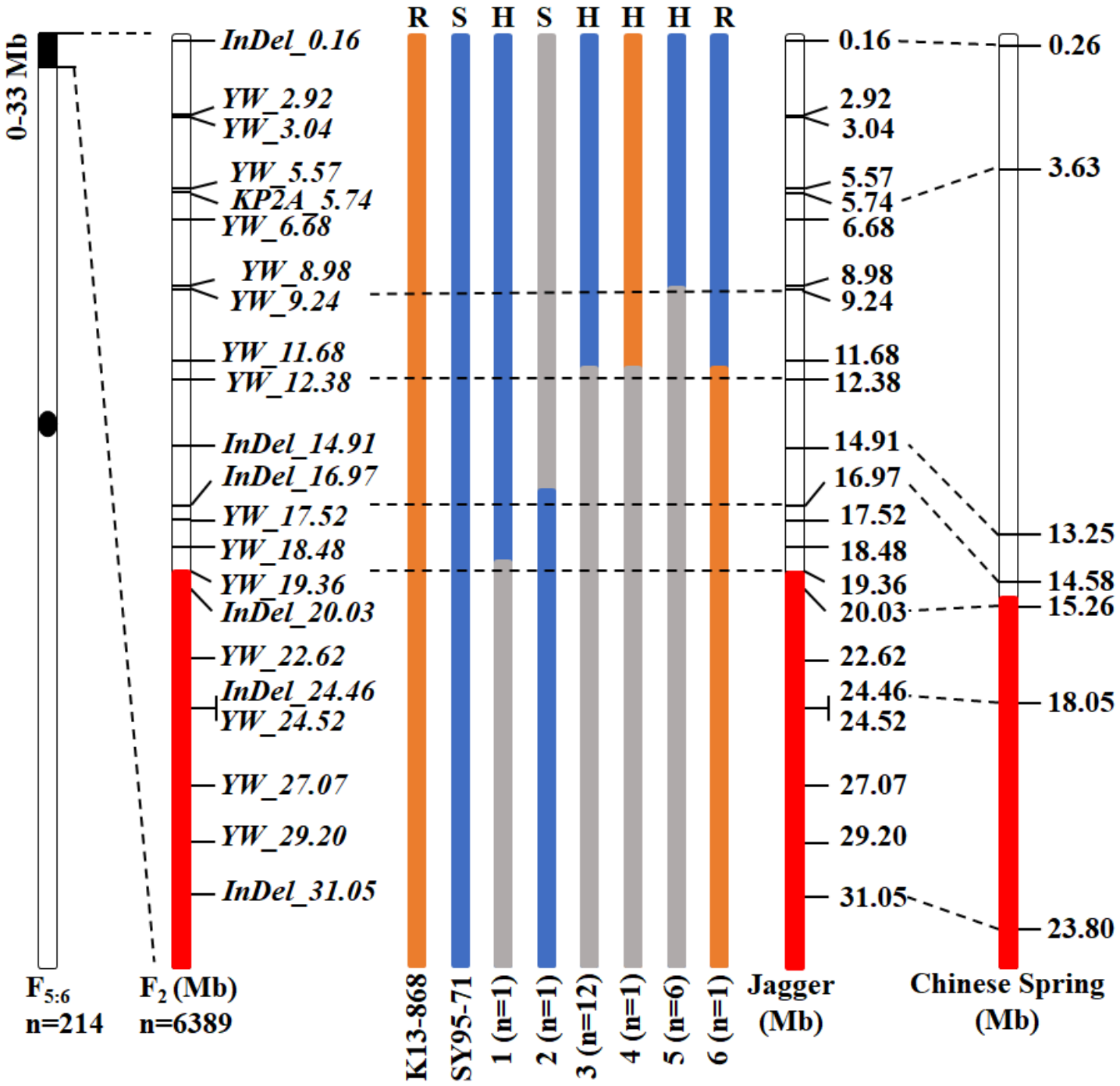

Figure 3

Fine mapping of the adult plant resistance gene to stripe rust in the *Aegilops ventricosa* 2N^{v}S segment. The genetic map was constructed with 22 markers genotyped on 6,389 plants, the physical map was based on the Jagger v1.1 genome and Chinese Spring v1.0 genome. The red boxes indicate the candidate gene region.

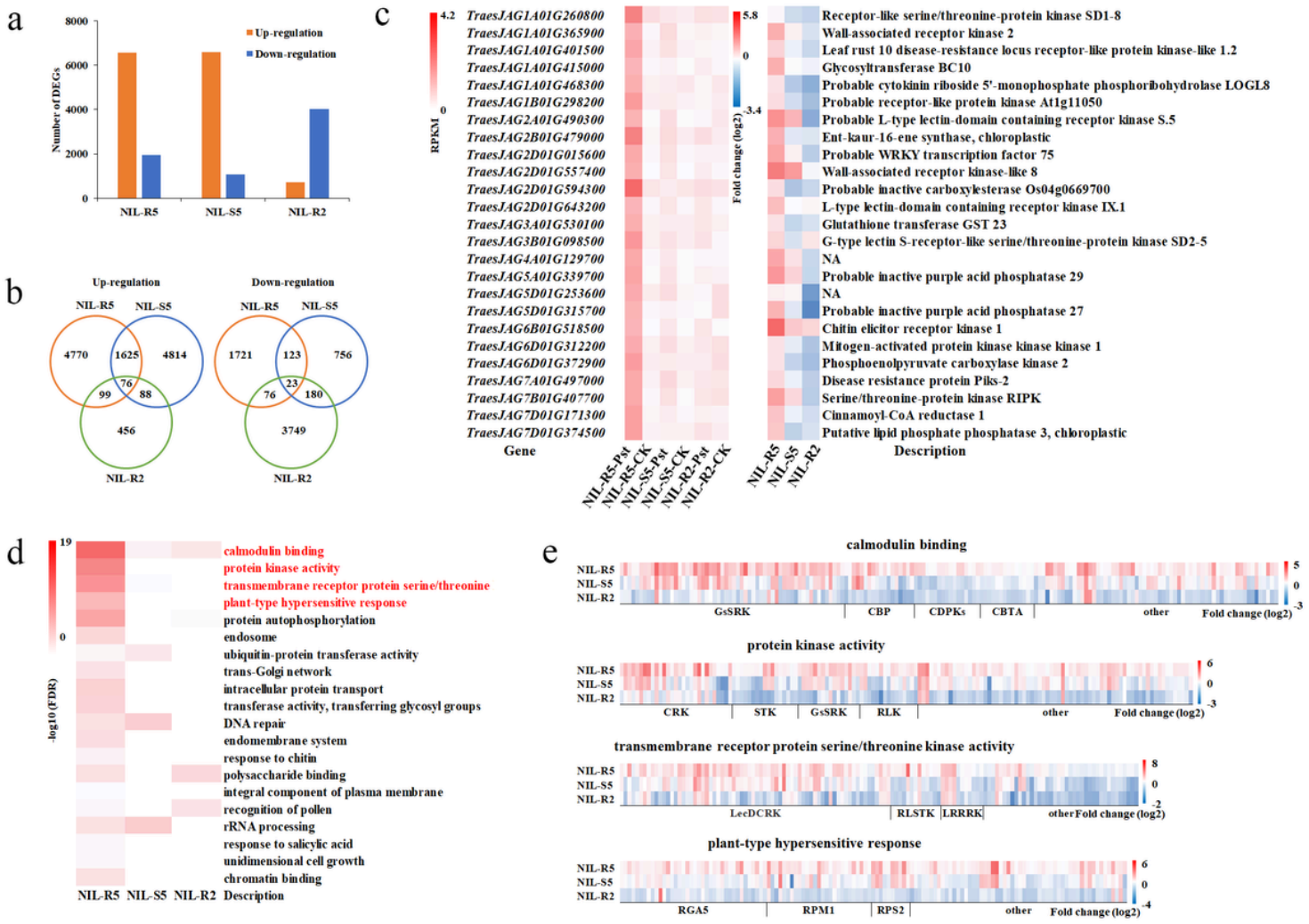

Figure 4

Transcriptome data from NIL-R and NIL-S. The number of up-regulated and down-regulated DEGs of the NILs after *Pst* infection at different stages (**a**). Venn diagrams showing the number of DEGs among the NILs after *Pst* infection at different stages (**b**). Heat maps showing the identical up-regulated DEGs were highly detected only in the inoculated NIL-R5 (**c**). GO annotation of DEGs, the top 20 significant enrichment GO terms were obtained in the upregulated DEGs in NIL-R5 (**d**). Expression of genes involved in calmodulin binding (GO:0005516), protein kinase activity (GO:0004672), transferase activity, transferring glycosyl groups (GO:0016757), and plant-type hypersensitive response (GO:0009626) in NIL-R5, NIL-S5, and NIL-R2 plants (**e**).

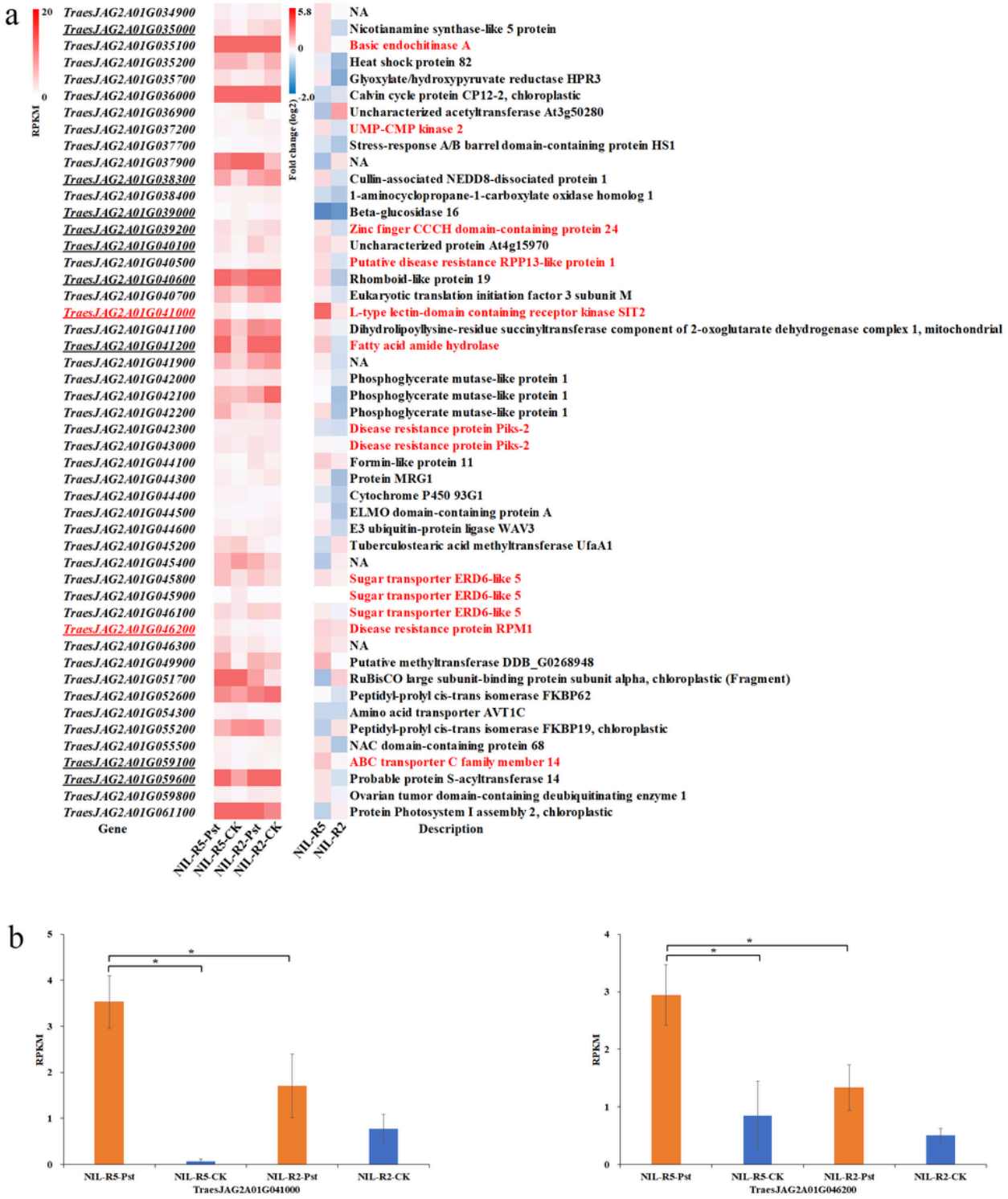

Figure 5

Heatmap of the 49 expressed genes identified within the candidate gene region (**a**), 13 gene annotations related to disease resistance are highlighted in red and 11 DEGs identified between mock and *Pst*infections at the adult plant stage of NIL-R were underlined. Two genes exhibited expression levels more than twice as high at the adult plant stage against *Pst* infection as at the seedling stage (**b**).

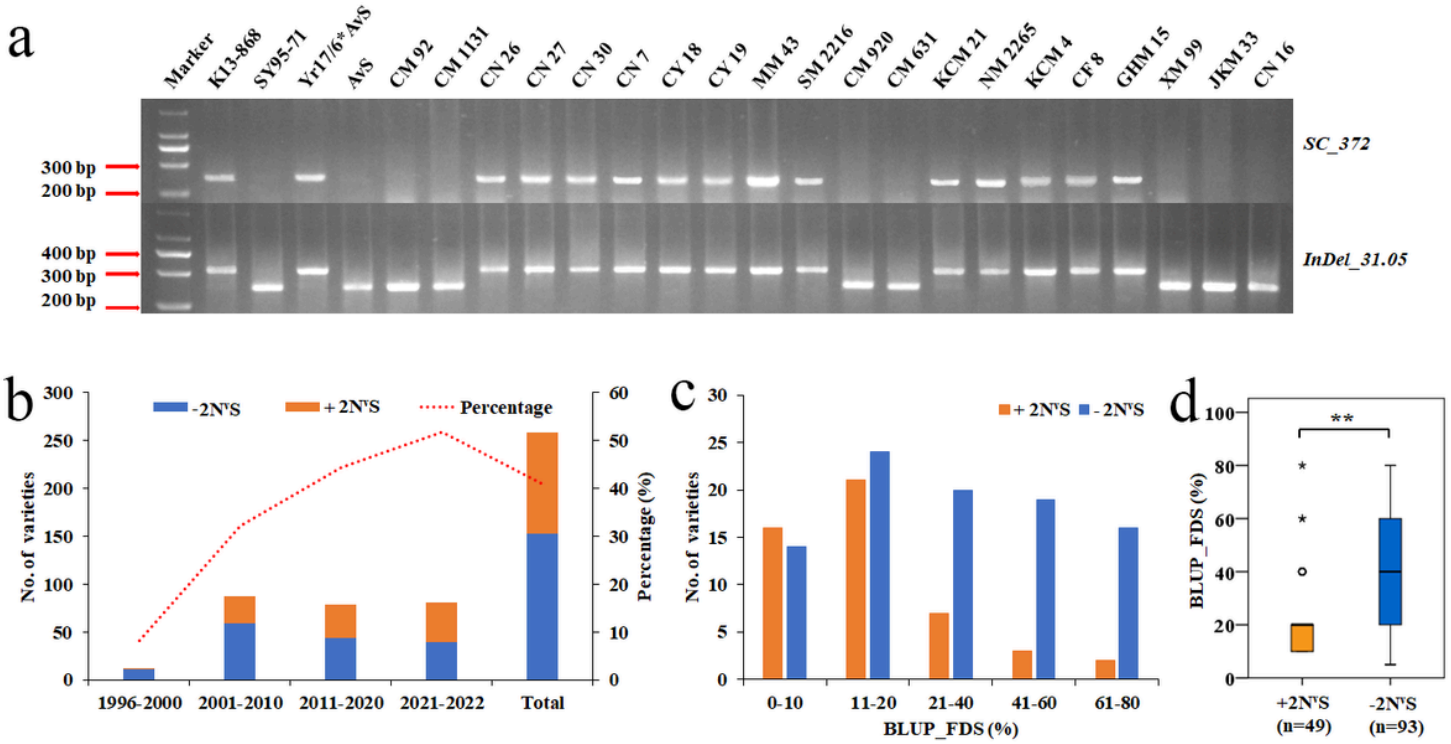

Figure 6

PCR profile in a set of wheat cultivars amplified by markers *SC_372* and *InDel_31.05* (**a**). Frequency distributions and percentage of varieties at four stages (**b**). Frequency distributions of the BLUP values of FDS of the varieties carrying the 2N^{v}S segment and without it (**c**). Boxplot displays the BLUP values of FDS of the varieties carrying the 2N^{v}S segment and without it (**d**).

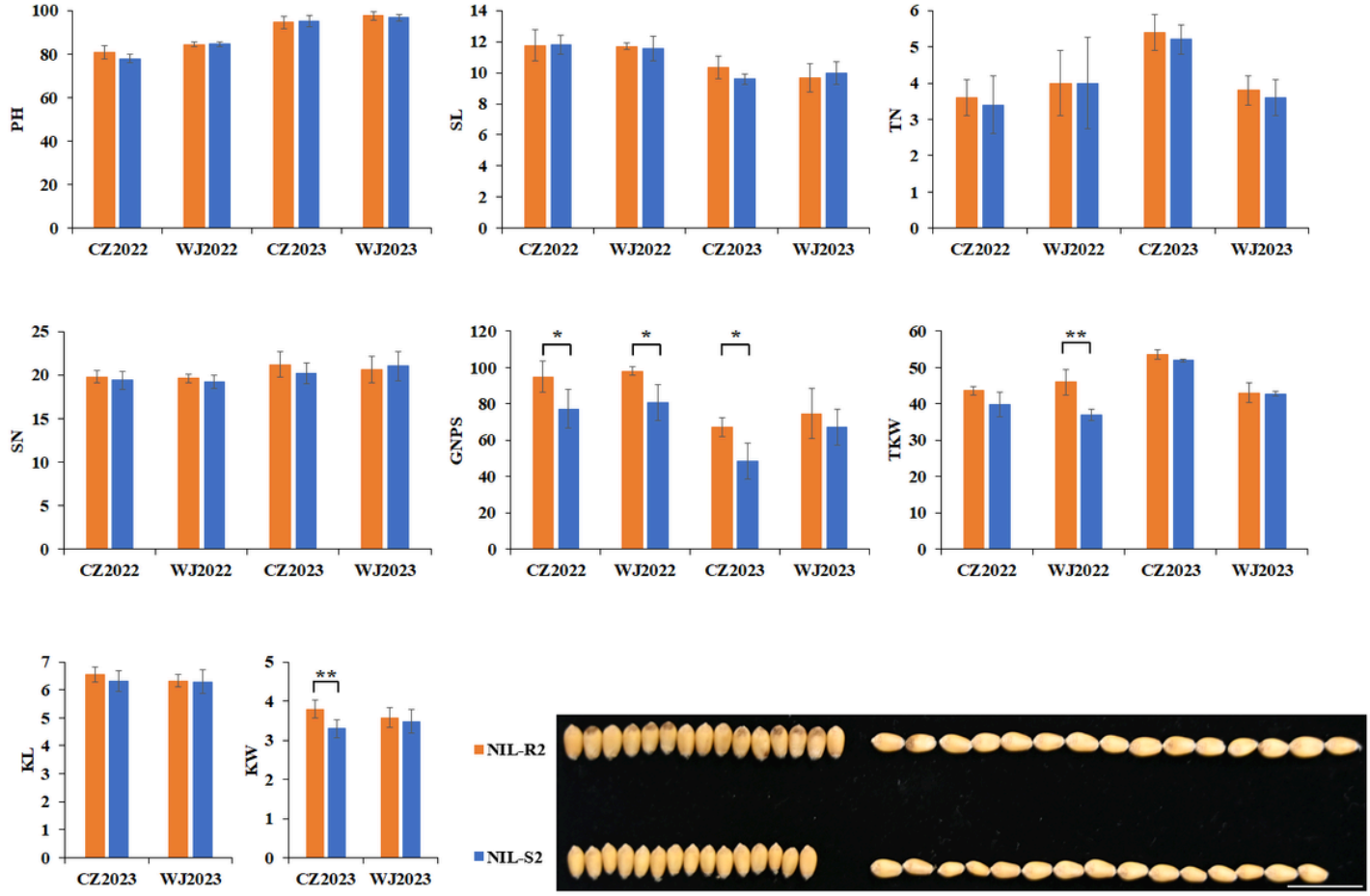

Figure 7

The agronomic traits of NIL-R and NIL-S plants shown by bar plots. CZ2022, Chongzhou 2022. WJ2022, Wenjiang 2022. CZ2023, Chongzhou 2023. WJ2023, Wenjiang 2023. PH, Plant Height. SL, Spike Length. TN, Tiller Number. SN, Spike Number. GNPS, Grain Number Per Spike. TKW, Thousand Kernel Weight. KL, kernel length, and KW, kernel width. **Significant at $P = 0.01$, *Significant at $P = 0.05$.

Supplementary Files

This is a list of supplementary files associated with this preprint. Click to download.

- Fig.S1.tif
- Fig.S2.tif
- Supplementarymaterials.xlsx